Translating Electronic Currents to Precise Acetylcholine-Induced Neuronal Signaling Using an Organic Electrophoretic Delivery Device

Klas Tybrandt, Karin C Larsson, Sindhulakshmi Kurup, Daniel Simon,
Peter Kjall, Joakim Isaksson, Mats Sandberg, Edwin Jager,
Agneta Richter-Dahlfors and Magnus Berggren

Linköping University Post Print

N.B.: When citing this work, cite the original article.

Translating electronic currents to precise acetylcholine–induced neuronal signaling using an organic electrophoretic delivery device**

By *Klas Tybrandt, Karin C. Larsson, Sindhulakshmi Kurup, Daniel T. Simon, Peter Kjäll, Joakim Isaksson, Mats Sandberg, Edwin W. H. Jager, Agneta Richter-Dahlfors*[*] and *Magnus Berggren*[*]

[*]   Prof. M. Berggren, K. Tybrandt, Dr. D.T. Simon, Dr. J. Isaksson, Dr. E.W.H Jager
        Organic Electronics, ITN, Linköping University
        SE-601 74 Norrköping, Sweden
        E-mail: magbe@itn.liu.se

        Prof. A. Richter-Dahlfors, K.C. Larsson, Dr. S. Kurup, Dr. P. Kjäll
        Department of Neuroscience, Karolinska Institutet
        SE-171 77 Stockholm, Sweden
        Agneta.Richter.Dahlfors@ki.se

        Dr. M. Sandberg
        Acreo AB, SE-602 21 Norrköping, Sweden

Biological systems are regulated by complex communication networks characterized by transduction of bio-signals between cells. The resulting cellular activity is specified by the chemical and conformational nature of the signal ion / molecule as well as its spatiotemporal patterning. The importance of such spatiotemporal regulation is well documented, *e.g.* in Ca^{2+} signaling.[1, 2] However, further understanding is hampered due to inherent limitations of current delivery techniques for controlled stimulation of biological systems. To overcome these problems, engineers have developed complex micro- and nano-fluidic systems, often made from glass or plastics.[3, 4] These may include an assortment of valves and pumps for the regulation of substance delivery.[5-9] Computer-controlled microfluidics for cell cultivation

1

and chemical signal generators for probing cellular dynamics show promising results for future investigation of cell signaling.[10, 11] However, microfluidic systems typically induce convection in the media, thereby altering the cellular microenvironment. In the worst case scenario, the liquid flow may cause detachment of surface-bound cells by mechanical forces.[12] It may also disturb any inherent chemical gradient of signaling molecules secreted by cells for cell-to-cell communication.[13] More subtle effects may also be introduced, as convection is known to cause shear stress that influences the biochemical behavior of cells, *e.g.* rearrangement of the cytoskeleton.[14]

Electronically controlled release systems can be a convection-free alternative to microfluidics. Silicon-based micro-reservoirs and –containers have been reported, in which the drug is released after electrochemical dissolution of a membrane.[15] For more dynamically controlled release of biomolecules, conjugated polymers have been evaluated. The softness, flexibility, and ion permeability of organic materials make them suitable for interfacing biological systems. Drug delivery electrodes based on conjugated polymers have been reported, in which the release is triggered by an applied potential causing electrochemical reactions within the conjugated polymer, thus releasing the electrostatically bound dopant ions.[16-20] Further, electronically controlled release from conducting-polymer nanotubes, fabricated on top of neuronal microelectrodes, have been demonstrated.[21] Although these devices have many attractive properties, they typically operate in a time interval of minutes to hours and there have been no reports on spatiotemporal delivery with dynamics in the range of seconds.

We recently reported an Organic Electronic Ion Pump (OEIP), which takes advantage of the combined electronic and ionic conductivity of conjugated polymers to deliver metal cations to cells under convection-free conditions. [22, 23] OEIPs with 50 to 4000 μm wide outlets were then utilized for delivery of K^+ to cells in concentrations above 50 mM. Because of residual ions in the channel, the delayed delivery time between addressing the pump and the induced cell responses was in the range of minutes. Here, we report on development of the OEIP

which has yielded *i)* expansion of the transport repertoire from metal cations to biomolecules, demonstrated by the neurotransmitter acetylcholine (ACh); *ii)* miniaturized outlets down to 10 μm channels, *i.e.* equal to or smaller than the size of individual neuronal cells; and *iii)* a reduction of the delay time of delivery, from minutes to seconds, by incorporating a preloading circuit which also minimized undesired delivery of residual ions. The above achievements result in exact correlation between the addressing signal and the delivery rate of ACh, enabling stimulation of single SH-SY5Y neuroblastoma cells via local [Ach] in the range of μM. Monitoring the induced Ca^{2+} responses we also demonstrate the electronic regulation of dynamic parameters, *e.g.* amplitude and frequency, and thereby the potential of this device to be used for further exploration of spatiotemporal patterning of cell signaling systems.

ACh is one of the major neurotransmitters in both the peripheral and central nervous systems where it effects *e.g.* synaptic plasticity and excitability.[24] Its positive charge across the range of physiological *pH* suggests that the chemistry of ACh would be compatible with the conducting polymer poly(3,4-ethylenedioxythiophene) doped with the polyanion poly(styrenesulfonate) (PEDOT:PSS) (**Figure 1a**). The principal device structure of the new 10μm-OEIP consists of three electrochemically active PEDOT:PSS electrodes and an SU-8 encapsulation incorporating openings for source (S), target (T) and waste (W) electrolytes (**Figures 1b, c**). The S, T, and W electrodes were linked by a channel system with dimensions varying between 10, 50, and 200 μm. This balances optimal throughput with high spatial resolution. Overoxidation of PEDOT:PSS in these channels renders the PEDOT phase permanently electrically insulating while leaving the ionic conductivity of the PSS phase unaffected.[25] Regions subjected to overoxidation serve as cationic exchange layers with substantially higher cationic than anionic conductivity. To achieve pumping of cations between two electrolytes the corresponding PEDOT:PSS electrodes are electrically addressed. The positively addressed electrode becomes oxidized while the negatively addressed electrode

becomes reduced.[26, 27] This creates an electric field forcing cations to migrate through the channel (**Figure 1d**). Typically, the source reservoir contained 40 μl of 0.1 M acetylcholine chloride, the waste reservoir 40 μl 0.1 M sodium chloride (NaCl), and the target reservoir contained cell medium, since this reservoir harbors the cells. Initially, the waste electrode was utilized for ACh loading of the channel by applying $V_{SW} = 20$ V for 3 min (SI 1). This scheme replaced the residual cations of the channel with ACh, which provides highly improved accuracy when delivering small quantities, compared to the previously reported OEIP.[22] After disconnecting V_{SW}, a voltage was applied to V_{ST} to initiate the migration of ACh from the source into the target electrolyte. The preloading procedure was shown to reduce the delivery delay time between addressing the 10μm-OEIP to actual ACh delivery from minutes down to a few seconds.

To investigate the transport characteristics of ACh through the 10μm-OEIP, different addressing times and voltages were applied. **Figure 2a** displays the delivered amount of ACh (mean values and standard deviations) for 10μm-OEIPs operated at $V_{ST} = 20$ V (*n*=3) and 40 V (*n*=3) together with representative electric currents vs. time. The electric current at 40 V is approximately twice as large as the current at 20 V. Furthermore, the current is stable over long periods of time and the measured amount of ACh in the target electrolyte increases linearly with time. Linear fits reveal that the delivery rate of ACh is 0.26±0.02 pmol s^{-1} and 0.55±0.03 pmol s^{-1}, for 20 V and 40 V respectively. The amount of ACh vs. the integrated current between the S and T electrodes, *i.e.* the transported charge, is given in **Figure 2b**. The linear slope gives a nearly constant transporting efficiency of 103±3% ($\Sigma n_{\text{ACh}}/\Sigma n_{\text{charge}}$) within a range of different addressing times and voltages. As each charge corresponds to one ACh molecule, the above results demonstrate the feasibility of using a conjugated polymer device to facilitate precision delivery of one of the most important signaling molecules in the nervous system, the neurotransmitter ACh.

Another important feature for delivery devices is the ratio between the delivery rate and spontaneous leakage, *i.e.* on-off ratio. In the PEDOT:PSS-based OEIP, active delivery is driven by migration while leakage is governed by diffusion. Recently, we reported an OEIP on-off ratio above 300 for alkali cations.[22] Here, leakage of ACh from the channel outlet into the target reservoir was found to be below the detection level of the measurement method used. However, assuming the Nernst-Planck equation applies, the drift vs. diffusion currents of ACh equals $J_{deliver} / J_{leak} = (F/RT) \cdot V_{ST} \approx 40V_{ST}$. Thus, for $V_{ST} = 10$ V the expected on-off ratio is 400. The on-off ratio can further be improved by applying a negative voltage between the waste and target electrodes in the off state.

The potential of the 10µm-OEIP for spatiotemporal delivery of ACh in cell signaling experiments was next explored in *in vitro* studies. In the nervous system, signaling agents such as ions (*e.g.* Ca^{2+}, K^+) and neurotransmitters are utilized to relay, amplify, and modulate signals. The human SH-SY5Y neuroblastoma cell line possess subtypes of the cholinergic ACh receptors, and has been widely used in a variety of Ca^{2+} signaling experiments for studies of voltage-dependent Ca^{2+} entry and receptor-mediated Ca^{2+} homeostasis.[28, 29] For a general overview of ACh-receptor induced Ca^{2+} responses, readers are referred to reference #30[30]. Microscopy-based real-time single-cell Ca^{2+} imaging of SH-SY5Y cells represents an ideal read-out system to monitor the cellular response to ACh. To enable accurate single cell stimulation *in vitro*, knowledge of local concentrations at a given time is crucial. We therefore modeled the evolution of the ACh concentration generated when biasing $V_{ST} = 5$ V from $t = 0$-100 s (**Figure 2c,** SI 2). This corresponds to an associated delivery rate of approximately 0.07 pmol s^{-1}. Hypothetically, a cell located 50 µm away from the outlet would be exposed to 140 µM ACh after 5 s, whereas at 150 µm the concentration would be 0.3 µM.

To test this hypothesis, we used SH-SY5Y cells as bio-sensors, since cholinergic ACh-receptor stimulation, using 10 µM ACh, is known to induce Ca^{2+} influx.[31] Cells cultivated on the target electrode were loaded with the ratiometric Ca^{2+} fluorophore Fura 2-AM (**Figure 1c**

and 2d). After pre-loading the 10μm-OEIP microchannel with ACh, baselines of intracellular Ca^{2+} levels were recorded. The low-intensity fluorescence, reflected by the steady baseline, reveals that the surface *per se* does not induce any Ca^{2+} response. By applying $V_{ST} = 5$ V, an increase in intracellular Ca^{2+} was rapidly observed in cells located within a radius of 50 μm from the channel outlet (**Figure 3a**). To characterize the evolving [ACh] at different distances from the channel outlet, we measured the time to half-maximal fluorescence intensity ($T_{max1/2}$) in cells. $T_{max1/2}$ in cells located >150 μm from the outlet showed delayed Ca^{2+} response with average $T_{max1/2} = 20$ s compared to $T_{max1/2} = 11$ s for cells <50 μm from the outlet (n = 3) (Figure 3a). This result validates the theoretically calculated [ACh] generated at various distances from the channel outlet (compare Figures 2c and 3a). Control experiments were performed with NaCl as source electrolyte to analyse whether activation of the pump triggers Ca^{2+} response. When Na^+, an ion that does not signal via the Ca^{2+} pathway, was transported at $V_{ST} = 20$ V, neither the electric field nor the potential induced any intracellular Ca^{2+} response (Figure 3b). However, SH-SY5Y cells responded promptly when ACh was added manually, using a pipette, into the target electrolyte (n = 3) (Figure 3b). The latter experiment demonstrates that the negative result of Na^+ transport is not a consequence of unhealthy cells. This series of experiments demonstrates that *i)* ACh can be transported through the PEDOT:PSS polymer; *ii)* transport through the polymer does not affect ACh's biological activity; and *iii)* electronic addressing of the 10μm-OEIP provides temporal control of delivered ACh molecules.

Dynamic parameters of biological signals, such as speed, amplitude, and spatiotemporal patterning, can be used to regulate diverse cellular processes.[32] We investigated whether the electronically controlled 10μm-OEIP can modulate dynamic parameters, such as amplitude and speed, of cellular Ca^{2+} signals. By applying $V_{ST} = 1$ V for 60 s, transported ACh elicited an intracellular Ca^{2+} response, which declined when V_{ST} was turned off (**Figure 3c**). When intracellular Ca^{2+} had returned to a lower fluorescence level, a second pulse of $V_{ST} = 10$ V was

applied for 60 s. This time, the Ca^{2+} response reached a substantially higher amplitude because of the 10-fold increase in applied V_{ST} (n = 5). Furthermore, varying the rate of ACh delivery, using 1 and 10 V, the dynamics of the Ca^{2+} transients can be electronically modulated, as indicated by the slopes. Figure 3c shows representative single-cell Ca^{2+} tracing, whereas the fluorescent read-out represented by an imaging sequence can be found in Supplementary Information (SI 3).

The device was then tested for its suitability to generate regular, oscillating Ca^{2+} signals in single cells exposed to temporally controlled release of ACh. By applying a high voltage (V_{ST} = 20 V) for a short time (<1 s), we hypothesized that a local increase of ACh would be generated that transiently activates individual cells. When ACh transport is interrupted, the high local [ACh] is expected to instantly collapse due to rapid diffusion of the neurotransmitter into the cell medium (SI 4). A typical response of SH-SY5Y cells exposed to an ACh pulse-train is presented in **Figure 3d**. The first pulse of delivered ACh (V_{ST} = 20 V for 0.2 s) rapidly induced a Ca^{2+} transient in cells located within 50 μm from the channel outlet, whereas cells located >150 μm away were unresponsive (n = 3). Thus, the spatial resolution of single cell stimulation is improved 5-fold compared to that previously reported.[22] Once intracellular Ca^{2+} had decreased to a lower fluorescence plateau, cells were exposed to the next ACh pulse, again resulting in a cellular Ca^{2+} transient. By repeating the procedure, a pulse train was generated with a temporal pattern mimicking that of naturally occurring Ca^{2+} oscillations (Figure 3d). This experiment also illustrates that the amplitude of the Ca^{2+} transient can be modulated by extending the time of applied pulses (0.2, 0.4, 0.6, 0.8, 1.0 and 2.0 s). In contrast to the shorter pulses, the longest pulse (2.0 s) resulted in a sufficiently high [ACh] to induce Ca^{2+} response also in the cell located > 150 μm away from the outlet.

The 10μm-OEIP presented here fulfills several important, previously unachievable requirements for cell signaling research. With this device, spatial resolution of individual cell stimulation in the range of 50-100 μm is achieved. Whereas the ionic conductivity of

conducting polymers in the OEIP previously has been utilized for transport of small (1-40 Da) cations (H^+, Na^+, K^+, Ca^{2+}), here we demonstrate the feasibility of this material for precise lateral transport of a positively charged, 146 Da biomolecule, the neurotransmitter ACh. The pre-loading circuit combined with the 10 µm-channel allows for fine-tuning of substance delivery, *i.e.* concentrations in the µM range can be precisely achieved. Parameterization of this all-solid state 10µm-OEIP device reveals excellent correlation between the electronic addressing signal, *i.e.* the current and voltage, and the associated delivery rate. We demonstrate the usability of these features for dynamic operation of the 10µm-OEIP, providing a means of controlling parameters involved in the spatiotemporal patterning of intracellular Ca^{2+} responses. Moreover, the 10µm-OEIP can be processed using standard photolithography and printing techniques that are easily integrated with other organic or inorganic solid-state systems. Taken together, this promises for further development of all-solid-state systems to create an interface where complex high-resolution signal patterns are generated to control cell physiology at the single cell and even sub-cellular level.

Experimental

Manufacturing of 10µm-*OEIPs.* The surface of PEDOT:PSS (AGFA-Gevaert Orgacon^TM F-350), coated on a polyethylene terephthalate substrate, was cleaned using 1112A remover (Shipley), then rinsed in acetone and deionized water. Shipley 1805 photoresist was deposited onto the PEDOT:PSS surface after pre-treatment with O_2-plasma and primer (hexamethyldisilazane). PEDOT:PSS was patterned using a O_2/CF_4 plasma etch-step. Overoxidized patterns of PEDOT:PSS were achieved by exposing the unsealed PEDOT:PSS areas to a sodium hypochlorite solution (1% (vol/vol), 20 s). Finally, a top layer of SU-8 2010 (MicroChem) was patterned on top of the electrode configuration and the target electrode was exposed to O_2 plasma etch through a plastic mask.

Measurement of ACh Transport. Devices were soaked in deionized water for 24 h prior to use. V_{ST} was applied with a Keithley 2602 source meter controlled via LabVIEW. The S electrolyte consisted of AChCl (40 µl, 0.1 M, Sigma ≥99% TLC) and NaCl (40 µl, 0.1 M) was used as T electrolyte. For each device, samples from T were collected after 100, 600, 1600, 3600, and 6600 s. The T electrode was repeatedly cleaned five times with a NaCl before a fresh electrolyte was applied. Collected samples were analyzed with an Amplex® Red Acetylcholine/Acetylcholinesterase Assay Kit (Molecular Probes).

Cell Cultivation. Human neuroblastoma SH-SY5Y cells (ATCC nr: CRL-2266) were propagated according to instructions from the supplier, in a 1:1 mixture of Eagle's Minimum Essential Medium (Sigma) and F12 medium (Sigma) supplemented to final concentrations of 10% fetal bovine serum (Sigma), L-glutamine (2 mM, Invitrogen), 1% non-essential amino acids (Sigma), penicillin (100 U ml-1, Sigma), streptomycin (0.1 mg ml-1, Sigma) and 1% Hepes (Sigma). Cells were propagated in 6 ml cell culture medium in tissue culture flasks (25-cm^2, Sarstedt), which were maintained in a humidified, 37 °C, 5 % CO_2 incubator, with the medium exchanged twice a week. At 80% confluency, cells were re-seeded at a ratio of 1:5. The night before the experiment, 10^5 cells (passage 6-20) were seeded on the target electrode in fresh medium. Water (Fischer Scientific, cell culture grade) was simultaneously placed on the remaining electrodes to hydrate the polymer over night.

Intracellular Ca^{2+} Recordings. To prepare cells for Ca^{2+} recordings, cells were incubated with the membrane-permeable Ca^{2+}-sensitive dye FURA-2 AM (2 µM, Molecular Probes) and 0.02% pluronic acid (Molecular Probes) in a humidified incubator (37 °C). After 1 h, Fura-2 AM was replaced with fresh cell media (50 µl). The 10µm-OEIP was prepared by applying ACh (50 µl 0.1 M, Fluka) as source electrolyte and NaCl (50 µl 0.1 M, Sigma) as waste electrolyte. Pre-loading of the transport channel was performed by applying V_{SW} = 20 V for 3

min. The basal level of intracellular Ca^{2+} was recorded before the ion pump was activated using potentials as described. Cells located at <50 μm and >150 μm away from the channel outlet were monitored using a Nikon TS-100 inverted microscope equipped with a 40 x /0.75 epifluorescence objective or an upright Nikon Eclipse 80i with a 40 x /0.80 epifluorescence objective. Excitation at 340 and 380 nm was achieved with a DeltaRAM illuminator and a DeltaRAM-V monochromator with a computer controlled SC500 shutter controller. Emission (510 nm) was collected every 4 or 8 s with a Photometrics Coolsnap CCD camera. Data were analyzed using PTI ImageMaster3 Software. $T_{max1/2}$ was calculated by subtracting the time at which the half maximum fluorescence intensity was reached after voltage application from the time at which the voltage was applied. Each set of experiments was repeated a minimum of three times, representative recordings are presented.

References

[1]   K. Mikoshiba, *J. Neurochem.* **2007**, *102*, 1426-1446.

[2]   M. J. Berridge, M. D. Bootman, H. L. Roderick, *Nat. Rev. Mol. Cell Biol.* **2003**, *4*, 517-529.

[3]   J. de Jong, R. G. H. Lammertink, M. Wessling, *Lab Chip* **2006**, *6*, 1125-1139.

[4]   J. M. K. Ng, I. Gitlin, A. D. Stroock, G. M. Whitesides, *Electrophoresis* **2002**, *23*, 3461-3473.

[5]   A. Brask, D. Snakenborg, J. P. Kutter, H. Bruus, *Lab Chip* **2006**, *6*, 280-288.

[6]   J. Noo Li, D. T. Chiu, C. J. Wargo, W. Hongkai, I. S. Choi, J. R. Anderson, G. M. Whitesides, *Biomed. Microdevices* **2002**, *4*, 117-121.

[7]   H. Suzuki, R. Yoneyama, *Sens Actuators B Chem* **2003**, *B96*, 38-45.

[8]   H. Xu, C. Wang, C. Wang, J. Zoval, M. Madou, *Biosens Bioelectron* **2006**, *21*, 2094-2099.

[9]   P. F. Pettersson, E. W. H. Jager, O. Inganas, presented at *1st Annual International IEEE-EMBS Special Topic Conference on Microtechnologies in Medicine & Biology*, Lyon, France, Oct 12-14, **2000**.

[10]   W. Gu, X. Y. Zhu, N. Futai, B. S. Cho, S. Takayama, *Proc. Natl. Acad. Sci. U. S. A.* **2004**, *101*, 15861-15866.

[11]   B. Kuczenski, W. C. Ruder, W.C. Messner, P.R. Leduc, *PLoS ONE* **2009**, *4(3)*, e4847.

[12]   X. L. Zhang, H. B. Yin, J. M. Cooper, S. J. Haswell, *Electrophoresis* **2006**, *27*, 5093.

[13]   V. V. Abhyankar, M. A. Lokuta, A. Huttenlocher, D. J. Beebe, *Lab Chip* **2006**, *6*, 389.

[14]   C. S. Chen, J. Tan, J. Tien, *Annu. Rev. Biomed. Eng.* **2004**, *6*, 275.

[15]   Y. Li, R. S. Shawgo, B. Tyler, P. T. Henderson, J. S. Vogel, A. Rosenberg, P. B. Storm, R. Langer, H. Brem, M. J. Cima, *J. Controlled Release* **2004**, *100*, 211-219.

[16]   L. L. Miller, *React. Polym., Ion Exch., Sorbents* **1986**, *6*, 341.

[17]   K. Kontturi, P. Pentti, G. Sundholm, *J. Electroanal. Chem.* **1998**, *453*, 231-238.

[18]   P. M. George, D. A. Lavan, J. A. Burdick, C.-Y. Chen, E. Liang, R. Langer, *Adv. Mater.* **2006**, *18*, 577-581.

[19]   M. Pyo, J. R. Reynolds, *Chem. Mater.* **1996**, *8*, 128-133.

[20]   R. Wadhwa, C. F. Lagenaur, X. T. Cui, *J. Controlled Release* **2006**, *110*, 531-541.

[21]   M. R. Abidian, D.-H. Kim, D. C. Martin, *Adv. Mater.* **2006**, *18*, 405-409.

[22]   J. Isaksson, P. Kjäll, D. Nilsson, N. Robinson, M. Berggren, A. Richter-Dahlfors, *Nat. Mater.* **2007**, *6*, 673-679.

[23]   J. Isaksson, P. Kjäll, D. Nilsson, N. D. Robinson, M. Berggren, A. Richter-Dahlfors, *Org. Electron.* **2008**, *9*, 303-309.

[24]   G. J. Augustine, D. Fitzpatrick, W. C. Hall, A.-S. LaMantia, J. O. McNamara, R. D. Mooney, M. L. Platt, D. Purves, S. A. Simon, L. E. White, S. M. Williams, in *Neuroscience,*

Fourth Edition, (Eds: D. Purves, G. J. Augustine, D. Fitzpatrick, W. C. Hall, A.-S. LaMantia, J. O. McNamara, L. E. White), Sinauer Associates InC, Sunderland Massachusetts **2008**, 90.

[25] P. Tehrani, N. D. Robinson, T. Kugler, T. Remonen, L.-O. Hennerdal, J. Hall, A. Malmstrom, L. Leenders, M. Berggren, *Smart Mater. Struct.* **2005**, *14*, 21-25.

[26] L. Groenendaal, F. Jonas, D. Freitag, H. Pielartzik, J. R. Reynolds, *Adv. Mater.* **2000**, *12*, 481-494.

[27] Q. Pei, G. Zuccarello, M. Ahlskog, O. Inganäs, *Polymer* **1994**, *35*, 1347-1351.

[28] R. J. Lukas, S. A. Norman, L. Lucero, *Mol. Cell. Neurosci.* **1993**, *4*, 1-12.

[29] D. G. Lambert, E. M. Whitham, J. G. Baird, S. R. Nahorski, *Mol. Brain Res.* **1990**, *8*, 263-266.

[30] F. Dajas-Bailador, S. Wonnacott, *Trends Pharmacol. Sci.* **2004**, *25*, 317.

[31] S. Fucile, M. Napolitano, E. Mattei, *Biochem. Biophys. Res. Commun.* **1997**, *230*, 501.

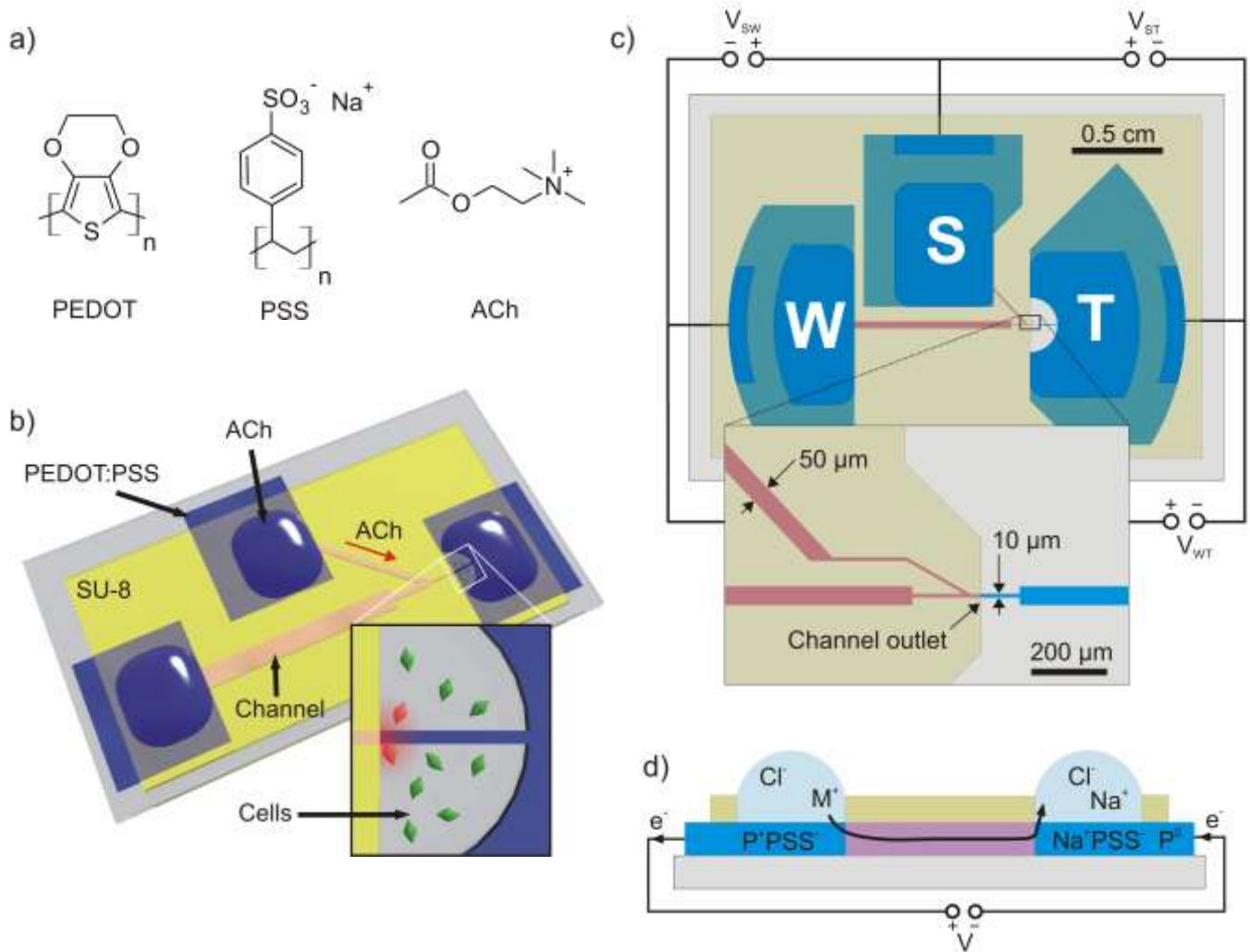[32] M. J. Berridge, P. Lipp, M. D. Bootman, *Nat. Rev. Mol. Cell Biol.* **2000**, *1*, 11-21.

Figure 1 The Organic Electronic Ion Pump. (**a**) Molecular structures of the conductive polymer PEDOT:PSS and the neurotransmitter ACh. (**b**) Overview of the 10μm-OEIP. The electrically conducting PEDOT:PSS electrodes are connected by cation selective polyelectrolyte channels. The SU-8 layer serves as insulation and encapsulation layer with defined openings for the electrolytes. ACh is transported through the channel and released locally into the cell culture. (**c**) Schematic top view of the 10μm-OEIP with addressing voltages. Electrodes are labeled source (S), target (T) and waste (W) according to their use. The zoomed area shows the 10 μm wide channel entering the target electrolyte at the SU-8 border. (**d**) Schematic cross section along the channel connecting two electrodes. The applied potential between the electrodes creates a closed electrochemical circuit, in which the electric current is compensated by an ionic current of the same magnitude through the channel. Thus the mobile cations M^+ in the target electrolyte are transported through the channel and immediately released into the source electrolyte due to the thinness of the channel (~200 nm). In this process, the source electrode is oxidized and the target electrode is reduced.
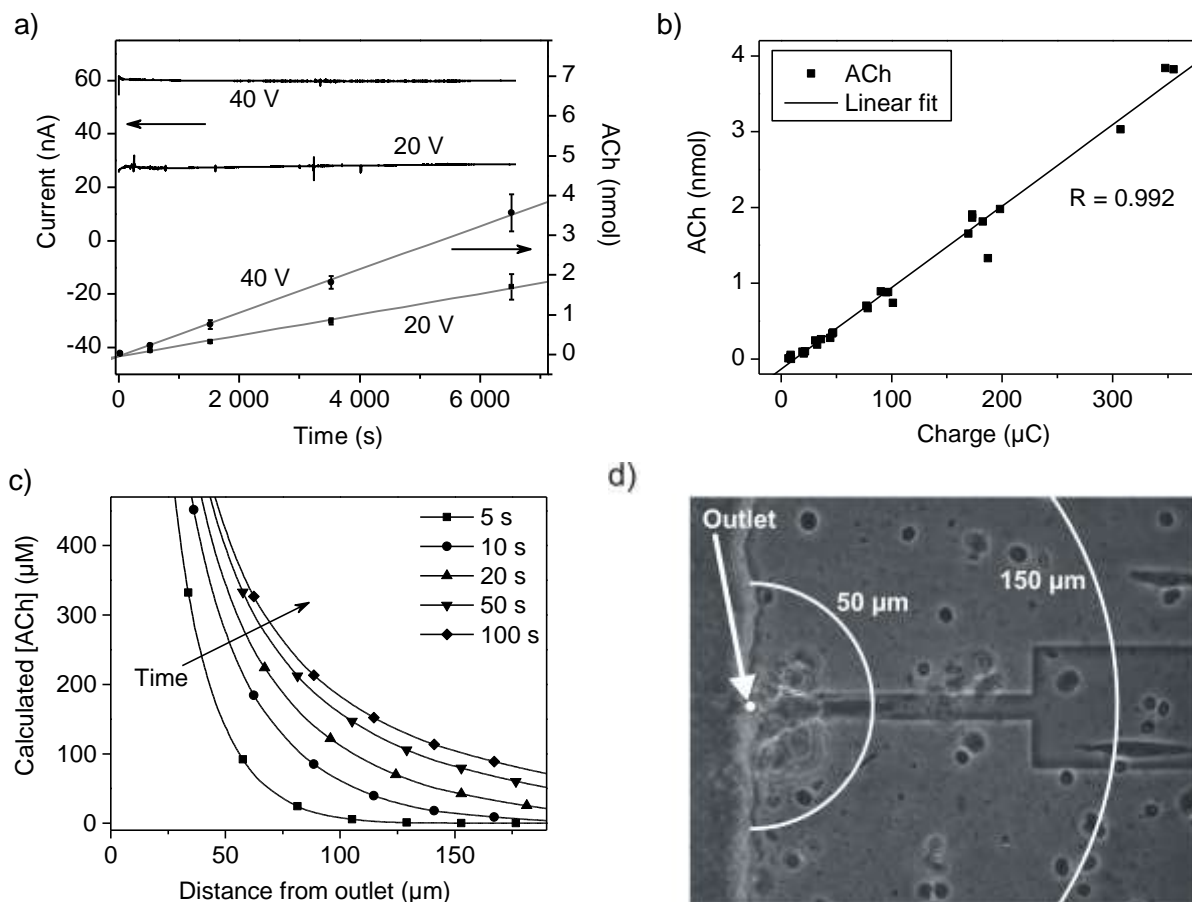
Figure 2 ACh transport in 10μm-OEIPs. **(a)** Characterization with V_{ST} set to 20 V and 40 V. The left axis shows the electric current from one 10μm-OEIP. The right axis shows the transported amount of ACh in the target electrolyte. Samples were collected from three 10μm-OEIPs at each voltage and the mean values, standard deviations and linear fits are shown. **(b)** Relationship between transported amount of ACh and integrated electric current. **(c)** Calculated evolution of [ACh] from the 10μm-OEIP outlet with V_{ST} set to 5 V at time zero. (d) Light microscope image of SH-SY5Y cells at various distances (50 and 150 μm) from the 10 μm channel outlet on the 10μm-OEIP.
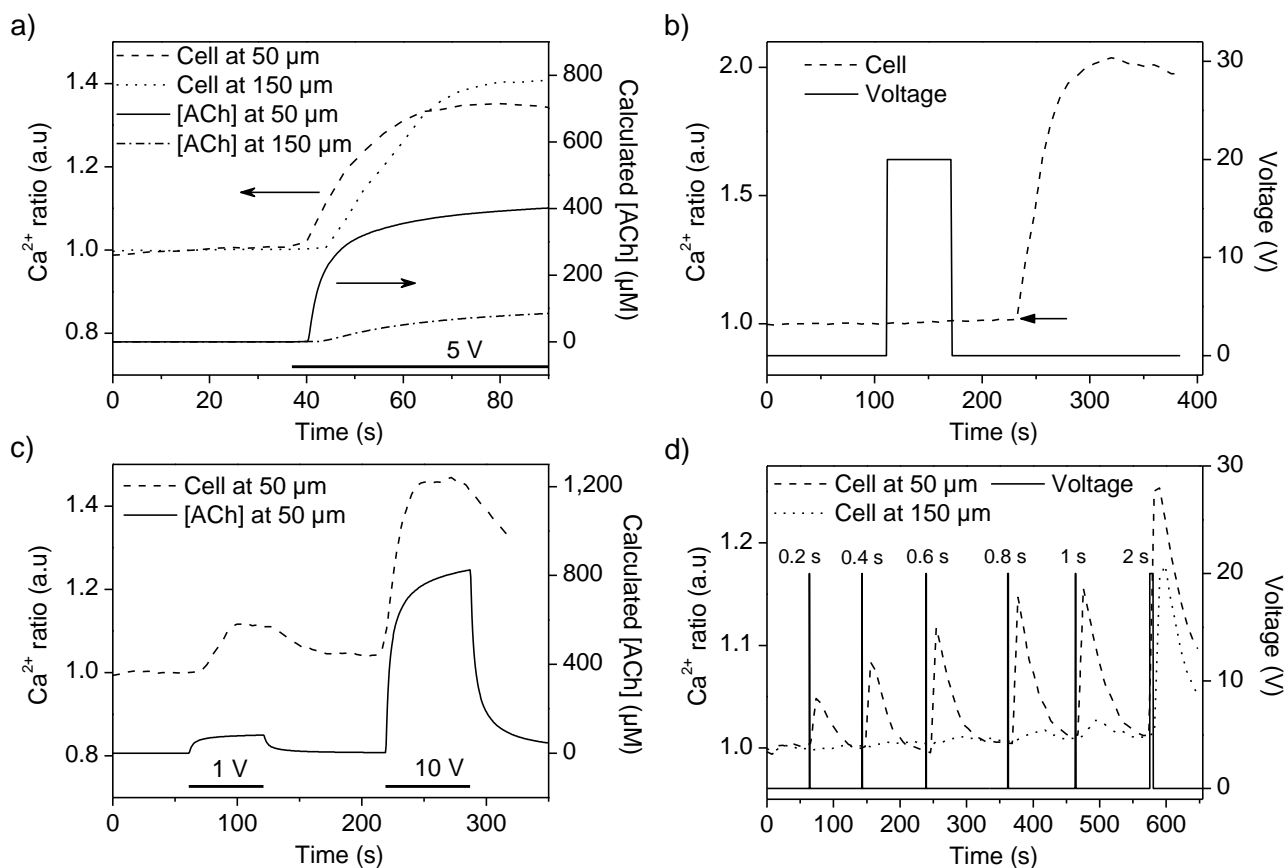
Figure 3 Intracellular Ca^{2+} recordings of SH-SY5Y cells. (**a**) Transport of ACh from source (0.1 M ACh) to target at $V_{ST} = 5$ V. Cells located <50 μm from the outlet respond immediately by an increase in fluorescence while a 9 s delayed response is observed in cells located >150 μm from the outlet. (**b**) Transport of Na^+ from source (0.1 M NaCl) to target at $V_{ST} = 20$ V. The arrow indicates manual addition of ACh to a final concentration of 1 mM in the target electrolyte. (**c**) The rate and amplitude of the Ca^{2+} responses can be modulated by applying 1 and 10 V for 60 s. (**d**) Applying a pulse-train of $V_{ST} = 20$ V for 0.2, 0.4, 0.6, 0.8, 1.0 and 2.0 s generates intracellular Ca^{2+} oscillations. The increasing pulse lengths are reflected in increased amplitude of the Ca^{2+} response. Short pulses result in high local [ACh] that induces local stimulation of single cells <50 μm while cells >150 μm from the outlet are non-responsive.

The table of contents entry :
A miniaturized organic electronic ion pump (OEIP) based on conjugated polymers is developed for delivery of positively charged bio-molecules. Characterization shows that applied voltage can precisely modulate the delivery rate of the neurotransmitter acetylcholine. The capability of the device is demonstrated by convection-free, spatiotemporally resolved delivery of acetylcholine via a 10 μm channel for dynamic stimulation of single neuronal cells.

Keyword (see list)
organic electronics, delivery, acetylcholine, spatiotemporal, neuronal signaling

Klas Tybrandt, Karin C. Larsson, Sindhulakshmi Kurup, Daniel T. Simon, Peter Kjäll, Joakim Isaksson, Mats Sandberg, Edwin W. H. Jager, Agneta Richter-Dahlfors[*], Magnus Berggren[*]

Title ((no stars))
Translating electronic currents to precise acetylcholine–induced neuronal signaling using an organic electrophoretic delivery device

ToC figure ((55 mm broad, 50 mm high, or 110 mm broad, 20 mm high))